Electronic Supplementary Information

Cucurbit[8]uril templated *H* and *J*-dimers of bichromophoric coumarin dyes: Origin of contrasting emission

Nilotpal Barooah,[1] Joytirmayee Mohanty[1,2] Achikanath C, Bhasikuttan*[1,2]*

[1]Radiation & Photochemistry Division
Bhabha Atomic Research Centre, Mumbai-400085, India
[2] Homi Bhabha National Institute, Anushaktinagar, Mumbai, INDIA

Materials and Methods

The bichromophoric coumarin derivatives namely 3-(2-Benzothiazolyl)-7-(N,N′-diethylamino) coumarin (Coumarin 6, C6), 3-(Benzimidazolyl)-7-(N,N′-diethylamino) coumarin (coumarin 7, C7) and 3-(2-N-methylbenzimidazolyl)-7-(N,N′-diethylamino) coumarin (coumarin 30, C30) were purchased from Aldrich and used without further purification. Cucurbit[8]uril (CB8) was synthesized and characterized following previously reported procedure. Commercially available CB8 from Aldrich was also used for some of the experiments. γ-Cyclodextrin used in the experiments is purchased from TCI. Nanopure water (Millipore Gradient A10 System; conductivity of 0.06 μS cm^{-1}) was used to prepare the sample solutions. $HClO_4$ as well as NaOH used for pH adjustment was obtained from Merck, India. pH measurements were carried out with Eutect Instruments P2700 pH meter at room temperature. Before measurements, pH meter was calibrated at pH 4, 7 and 10 with pH standard buffers provided by Eutect Instruments Ltd. Since C7 and C30 are sparingly soluble in water at pH >4, for optical absorption and emission measurements, the dye samples were dispersed in water at pH3 and stirred vigorously for two hours at room temperature. The mixtures were then centrifuged and centrifugates were collected. which were finally filtered again and diluted with water at pH 3 before carrying out spectroscopic measurements. The maximum achievable concentration for C7 and C30 dyes in pure aqueous medium at pH 3 were found to be ~16μM and ~55μM respectively. In case of C6 dye, ethanolic solution of the dye was added to aqueous 0.05M $HClO_4$ solution with stirring to get red coloured precipitate. The precipitate was collected after centrifugation and dispersed in 10ml of aqueous 0.05M $HClO_4$. The dispersion was stirred for about 1h and centrifuged again to remove the undissolved part. The homogeneous aqueous solution was left undisturbed overnight, which was finally centrifuged again and diluted with water and adjusted the pH.

Steady-state UV-visible and Fluorescence Spectroscopy: UV-visible spectroscopic measurements were carried out in aqueous solution with 10mm path length quartz cuvette. Absorption spectroscopic measurements were carried out at 25°C using Jasco V-650 model (Japan) UV-vis spectrophotometer. Steady-state emission measurements were carried out using a Hitachi (Tokyo, Japan) model F-4500 spectrofluorimeter. The samples were excited at specific wavelengths (preferably at isosbestic point) to maintain minimum change in the absorbance in the presence of host and the small changes if any, have been corrected.

Time-resolved emission measurements: Time-resolved fluorescence measurements were carried out using a time-correlated-single-photon-counting (TCSPC) setup (IBH, UK). In the present work, 451 nm diode laser (~100 ps, 1 MHz repetition rate) was used as the excitation source and a microchannel plate photomultiplier tube (MCP-PMT) was used for fluorescence detection. A re-convolution procedure was used to analyze the observed decays using a proper instrument response function obtained by substituting the sample cell with a light scatterer (suspension of TiO_2 in water). With the present setup, the instrument time resolution is adjudged to be better than 50ps. The fluorescence decays were analyzed as a sum of exponentials as,

$$I(t) = \sum_i B_i \exp(-t/\tau_i) \qquad \text{(S1)}$$

where, $I(t)$ is the time dependent fluorescence intensity and B_i and τ_i are the pre-exponential factor and the fluorescence lifetime for the i^{th} component of the fluorescence decay. The quality of the fits and consequently the mono or bi-exponential nature of the decays was judged by the reduced chi-square (χ^2) values and the distribution of the weighted residuals among the data channels. For an acceptable fit, the χ^2 value was close to unity and the weighted residuals were distributed randomly among the data channels.

^{1}H-NMR measurements: The ^{1}H-NMR experiments were performed in D_2O (99.8%) using Varian 600 MHz HCN-Cryoprobe spectrophotometer at National NMR Fcility, TIFR, Mumbai, India. Because of the very low solubility of the dyes in D_2O at neutral pH, the NMR experiments could be carried out only at pD 3 with minimum 1000 scans per spectra. For ^{1}H-NMR titrations the pD values of the solutions were adjusted by addition of DCl (32% in D_2O) to D_2O and C7 / C30 and the solutions were prepared following the same procedure described before. However, probably due to the concentration restrictions, the 1D NOESY and 2D ROESY experiments attempted remained inconclusive.

Mass spectrometric measurements: Electrospray ionization mass spectrometric (ESI-MS) measurements of the host-guest complexes were carried out with Bruker Daltonic model microTOF-QII instruments in positive ion mode at capillary Voltage of -4500V and the dry gas temperature was 180°C. Aqueous samples with ≤1μM concentration at preset pH 3 was diluted with acetonitrile:water (at pH3) mixture (30:70 v/v) and samples were injected at a rate of 3μL per minute. Additionally, some of the measurements were carried out with Bruker Impact^{TM}-TOF mass spectrometer.

Isothermal titration calorimetry (ITC): Isothermal titration experiments were carried out on a iTC_{200} MicroCalorimeter from Microcal GE Healthcare, Inc. Hong Kong at 25°C in water at pH3. The titrations were performed using dye (C30 and C7 dyes) concentration of 5μm to which CB8 (90μM) solution at pH3 was titrated. Typically 20 consecutive host injections of 2 μL each were used. All solutions were degassed prior to titration. Heats of dilution were determined by titrating the CB8 solution into water at pH3 and were subtracted from the observed titration data. The first two data point was removed from the data set prior to curve fitting. The data was analyzed with Origin 8.0 software with the two set of sites model. The complex binding constant (K_a) and molar

reaction enthalpy (ΔH^o) are used in the calculation of standard free energy (ΔG^o) and entropy changes (ΔS^o) according to the equation $\Delta G^o = -RT \ln K_a = \Delta H^o - T\Delta S^o$.

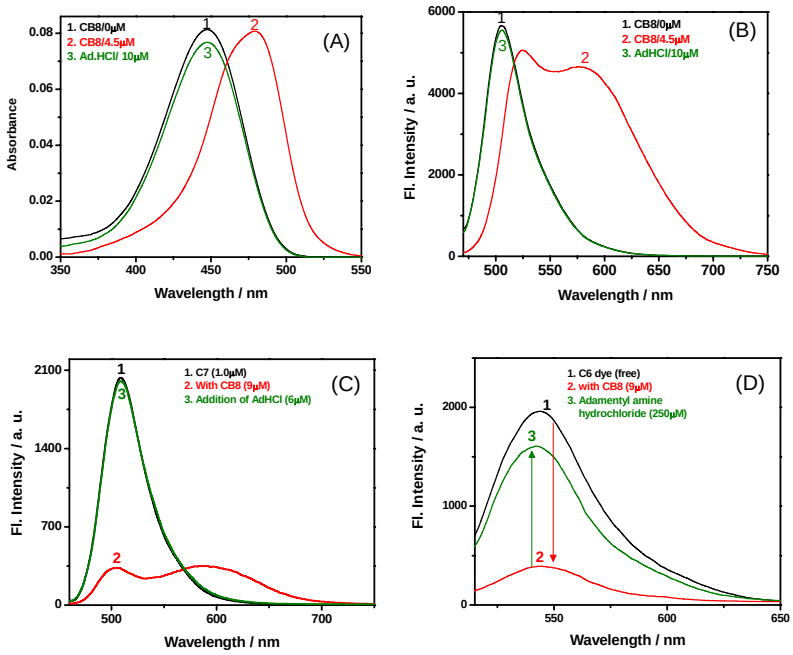

Fig.S1: Steady-state Absorption (A) and Emission (B) spectroscopic profile of free C30 dye (1), in presence of 4.5μM CB8 (2) and solution (2) with 10μM of adamentyl amine hydrochloride (3). Spectrum (C) and (D) shows the fluorescence recovery recorded on addition of adamentyl amine hydrochloride to the CB8-C7 and CB8-C6 systems respectively.

Note S1: *Time resolved emission spectroscopic studies of monocationic C30, C7 and C6 dyes in presence of CB8 :*

Effect of interaction with CB8 host on the excited state decay kinetics of the bichromophoric coumarin dyes namely C6, C7 and C30 were studied by time correlated single photon counting (TCSPC) technique. The comparative decay profiles of these guest dyes in free and in presence of CB8 under experimental pH conditions are shown in Fig.S2.

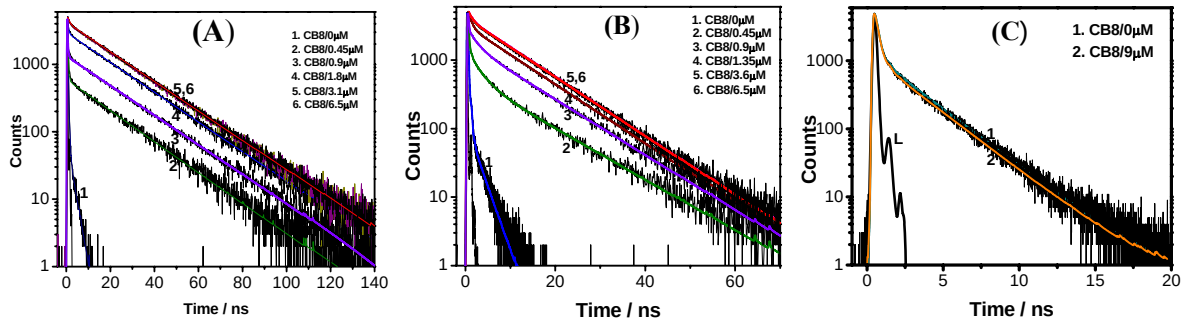

Fig.S2: Excited state decay kinetics of (**A**) free C30 dye and in presence of increasing CB8 host concentration; (**B**) for free C7 dye and in presence of increasing concentration of CB8 host and (**C**) free C6 dye (1) and in presence of CB8 (2); all system at pH 3

At pH 3, in strongly hydrogen bonding aqueous environment, C30 displays fast decay kinetics with major contribution from a lifetime component of 0.13ns (96%) along with a negligible long decay component of 2.3ns (4%) manifesting the intramolecular charge transfer character of the monocationic form of C30 dye in the excited state. As shown in Fig.S2(A), with increase in the concentration of CB8 host, the excited state decay kinetics of C30 dye displayed unprecedented long lifetime of 19.7ns (98%) with a minor contribution from a short component of 0.15ns (2%). In a similar way as shown in Fig.S2(B), C7 dye displayed fast decay kinetics in aqueous solution at pH3 with major lifetime component of 0.18ns (90%) along with a relatively long component of 2.26ns (10%). At low CB8 concentration (≤1μM), the decay kinetics of C7 dye displayed a complex profile following a tri-exponential decay pathway most probably, due to the involvement of multiple host-guest equilibrium processes in solution. With gradual increase in concentration of CB8, the decay dynamics of C7 dye became increasingly slower which finally display a lifetime of 10ns (98%) with negligible contribution from a short decay component of 0.7ns (2%) in presence of 3.6μM of CB8 which remained unaltered with further increase in CB8 concentration. Table S1(A) & S1(B) summarizes the decay time constants measured for C30 and C7 dyes respectively under different experimental conditions.

Table S1 (A): *Excited state decay constants of C30 dye with increasing CB8 concentration in aqueous solutions at pH3.*

Concentration of CB8 Host (in μM)	Lifetime (ns) (% contribution)		
	τ_1	τ_2	χ^2
0	0.13 (96)	2.36 (4.0)	1.18
0.45	0.16 (21)	19.76 (79)	1.12
0.90	0.18 (9)	19.76 (91)	1.11
1.80	0.33 (3)	19.76 (97)	1.11
3.10	0.65 (2)	19.76 (98)	1.10
6.50	0.76 (2)	19.76 (98)	1.06

Table S1 (B): *Excited state decay constants of C7 dye with increasing CB8 concentration in aqueous solutions at pH3*

Concentration of CB8 Host (in μM)	Lifetime (ns) (% contribution)			
	τ_1	τ_2	τ_3	χ^2
0	0.17 (89)	----------	2.30 (11)	1.17
0.45	0.17 (23)	1.50 (13)	10.00 (64)	1.17
0.90	0.17 (8)	1.50 (8)	10.00 (84)	1.11
1.35	0.60 (7)		10.00 (93)	1.14
3.60	0.70 (2)		10.00 (98)	1.05
6.50	0.70 (2)		10.00 (98)	1.06

Note S2: *Jobs plot for determination of host-guest complex stoichiometry for CB8.C30 and CB8.C7 systems*

Jobs continuous variation method was applied to determine the complex stoichiometry of CB8-C30 and CB8-C7 host-guest systems by varying the concentration of the host and the guest, while keeping the total concentration same in aqueous solutions at pH 3. Steady-state spectroscopic features were measured by either applying UV-vis. absorption or emission spectroscopic methods. For CB8.C30 host-guest system, Jobs plot was constructed by monitoring absorbance at 480nm, the wavelength where the existing host-guest complex has predominant absorption. The measured absorbance at this wavelength is further corrected for free dye contributions at particular mole fraction of the dye and was plotted against the mole fraction of the dye, η(dye). Similarly, in case of CB8.C7 system, the emission intensity at 630nm (λ_{ex} 460nm) was plotted against the mole fraction of the dye. The free C7 dye has no emission at 650nm and therefore, the observed emission intensity changes were measured at 550 nm. As shown in the inset of Fig.1A, B, both the CB8.C30 and CB8.C7 host-guest systems showed clear inflexion point at 0.4 which indicates a 3:2 CB8:C30/C7 stoichiometry, respectively. For the CB8.C6, however, the system displayed the inflection point at ~0.66 (inset, Fig.1C), corresponding to a 1:2 stoichiometry.

Note S3: *^{1}H-NMR spectroscopic studies on interaction of C30, C7 and C6 dye with CB8 host in D_2O at pD3*

^{1}H-NMR spectroscopic measurements were carried out for free C30, C7 and C6 guest dye molecules and in presence of CB8 host to elucidate the binding site and stoichiometry of the host-guest complexes in D_2O at pD3. All these guest molecules displayed pronounced complexation induced NMR shifts of various proton resonances. All

experiments were performed at room temperature in D_2O at pD3. The details of each set of experiments are discussed below.

a) Interaction of C30 dye with CB8 host

Coumarin 30 dye exists as monocationic form with protonation at the N-methylbenzimidazole unit in D_2O at pD3. As shown in the Fig.S3, the aromatic protons coumarin core in free C30 dye namely, H_a, H_b, H_c and H_d appear at δ 6.67 (s, 1H), 7.54 (d, *J*= 6Hz, 1H), 6.85(d, *J*= 6Hz, 1H) and 8.32 (s, 1H) along with the protons from N-methylbenzimidazole unit, H_e and H_h at δ 7.76 (d, *J*= 6Hz, 1H) and 7.72 (d, *J*= 6Hz, 1H) and H_f and H_g appear together as a broad multiplet at δ 7.56 (bm, 2H). The aliphatic protons-NCH_3 substituent on the benzimidazole unit appeared at δ 3.96 (s, 3H) and that of 7-N,N′-diethylamino group on the coumarin core appeared at δ 3.47 (q, J_{12}= 6Hz, 4H) and 1.14(t, J_{12}= 6Hz, 6H).

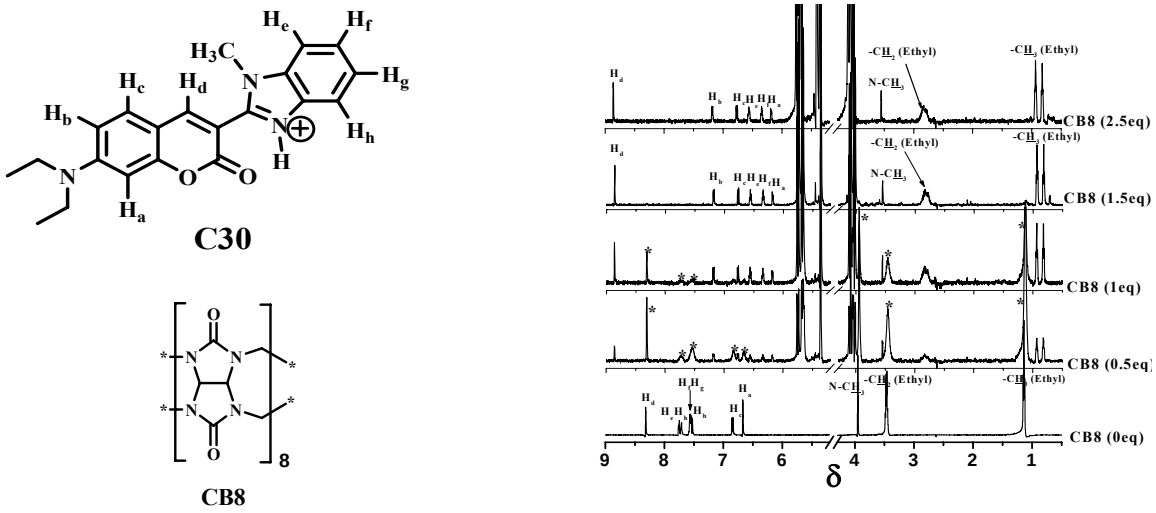

Fig.S3 ^{1}H NMR titration for C30 (50μM) with CB8 host dye in D_2O at pD3

Addition of 0.5 eq. of CB8 host led to significant broadening of aromatic proton resonances and the spectra displayed signals of CB8 encapsulated as well as free protons of C30 molecule. In the aliphatic part two set of –NCH_3 singlets were observed at δ 3.96 and 2.61 originating from the free and the bound dye respectively. Similarly, –CH_2 groups of 7-N,N′-diethylamino substituent appeared at δ 3.47 and 2.80 and the –CH_3 groups appeared as a set of singlets at δ 0.94 and 0.84 along with prominent signal at it original position at δ 1.14. Increase in concentration of the CB8 host to 1.5 eq. led to complete disappearance of the free dye signals and displayed impressive complexation induced shifts of all proton resonances of C30 molecule. At this CB8 concentration all the dye molecules are present as host-guest complex where, the aromatic protons of coumarin core namely H_a, H_b and H_c displayed 0.49, 0.35 and 0.09ppm upfield shift to their new positions at δ 6.19 (d, *J*= 6Hz, 1H) and 7.19 (d, *J*= 6Hz, 1H) and 6.76 (d, *J*= 6Hz, 1H) indicating that these protons are embedded inside the hydrophobic cavity of CB8 host. Quite interestingly, only two set of broad signals were observed for the N-methyl benzimidazole protons namely, H_e, H_f, H_g and H_h at δ 6.56 and 6.35, each of which were integrated to one proton. Considering the large cavity size

of CB8 host capable of encapsulating two aromatic units such as benzimidazole, we anticipated that two C30 molecules might interact with one CB8 host through encapsulation of the *head-to-tail* stacked N-methylbenzimidazole moieties of two guest dyes where the N-methyl groups are facing opposite directions. This configuration eventually renders magnetic equivalence of the aromatic protons N-methyl benzimidazole units leading to only two sets of non-equivalent aromatic protons namely H_e/H_h and H_f/Hg. These protons because of their complete encapsulation inside CB8 cavity, displayed impressive 1.00 and 1.21ppm upfield shift compared to their original free dye resonance positions in the ^{1}H-NMR spectra. Consequently, the N-methyl group also displayed 1.35ppm upfield shift and appeared at δ 2.61 indicating its inclusion inside the CB8 cavity. However, comparing the size of the C30 dye and the length of the CB8 host cavity it is difficult to explain the observed complexation induced NMR shifts for the aromatic protons of coumarin end as well as for the –CH_2CH_3 protons of 7-N,N′-diethylamino substituent. The –CH_2 protons from two ethyl groups appears as a broad signal at δ 2.84 with 0.54ppm upfield shift and the two –CH_3 protons shows two clear triplets at δ 0.94 and 0.84 with an average of 0.25ppm upfield shift compared to their free dye positions. Therefore, with the anticipated 1:2 CB8.C30 complex stoichiometry, we considered further interaction of two CB8 host from both the coumarin ends that encapsulates the 7-N,N′-diethylamino group and partly the coumarin ring. Most interestingly, this structural arrangement of the host and the guest molecules places the coumarin-H_d protons in the deshielding region of the carbonyl portals of two CB8 host molecules and thereby, explains the contrasting 0.54ppm downfield shift observed for H_d protons appearing at 8.86 (s, 1H). Based on these NMR spectroscopic evidences, we accepted a 3:2 CB8.C30 host-guest complex stoichiometry supporting the stoichiometry observed in the Jobs plot for the same.

b) Interaction of C7 and C6 dye with CB8 host

In presence of CB8 host C7 also displayed complexation induced NMR shifts in D_2O at pD3 but in a different way. Because of low concentration of C7 dye in the experimental pH conditions, titration experiments with CB8 host remained inconclusive because of considerable broadening and disappearance of signals. However, in presence of excess amount of CB8, C7 displayed well resolved signals as shown in the Fig. S4,B and was compared with the free dye spectra of C7 (Fig. S4A). In a similar way of C7 dye, all aromatic protons of C6 dye displayed large upfield shift in presence of CB8 with respect to their free dye positions (Fig. S4, C&D). However, complete identification of all aromatic proton resonances could not be made as most of the signals overlapped and as well as because of the low signal intensity due to insufficient concentration. Interestingly, the –CH_2 and –CH_3 protons from 7-N,N′-diethylamino group did not show any complexation induced shift ruling out their inclusion inside CB8 cavity.

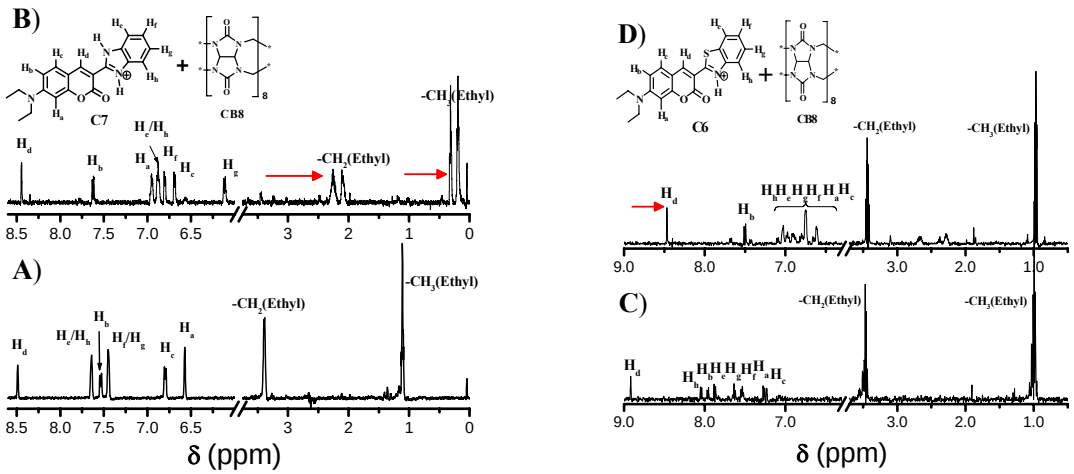

Fig.S4 ^{1}H NMR titration for C7 in the absence (A) and presence of CB8 (B) in D_2O at pD3. ^{1}H NMR titration for C6 in the absence (C) and presence of CB8 (D) in D_2O at pD3.

Note S4: *ESI-TOF mass spectrometric measurements of $(C30)_2$-CB8 complex:*

ESI-TOF mass spectrometric measurements were attempted with all the three solutions of C30, C7 and C6 dyes in presence of CB8 host in aqueous solution at preset pH 3. Despite of many attempts, we were only successful to obtain the indication for CB8-$(C30)_2$ and CB8-$(C7)_2$ complexes in solution which are shown below. Mass spectrometric (ESI-TOF) studies on CB8-C30 system (Fig.S5A) in acidic aqueous-acetonitrile (60/40; v/v) at pH 3, rendered peak at m/z 506.4, along with signals for host CB8, which is assigned to $[(CB8.H^{2+})\mathbf{.}(C30H^{+})_2]^{4+}$ complex (calculated m/z 506.7), corresponding to the 1:2 stoichiometry. In case of CB8-C7 system (Fig. S5B), the signal at m/z 1000.79 was assigned to $[CB8{:}(C7H^{+})_2]^{2+}$ (calculated m/z 1000.66) in agreement with a 1:2 stoichiometry.

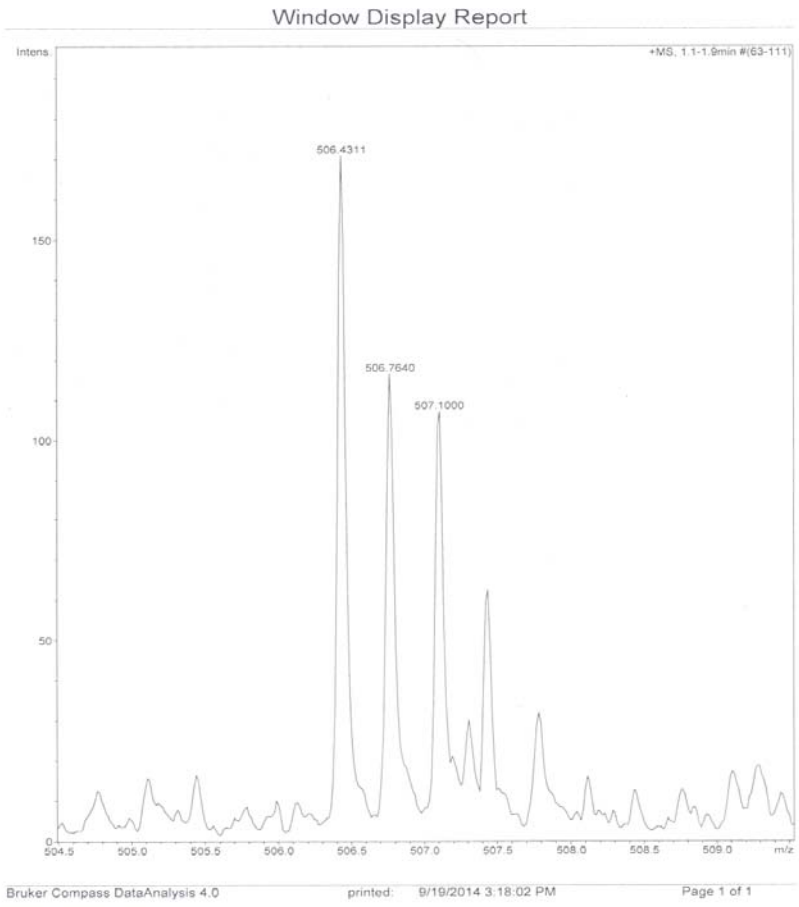

Fig.S5A: Mass spectroscopic data for the CB8-C30 system in solution at pH 3

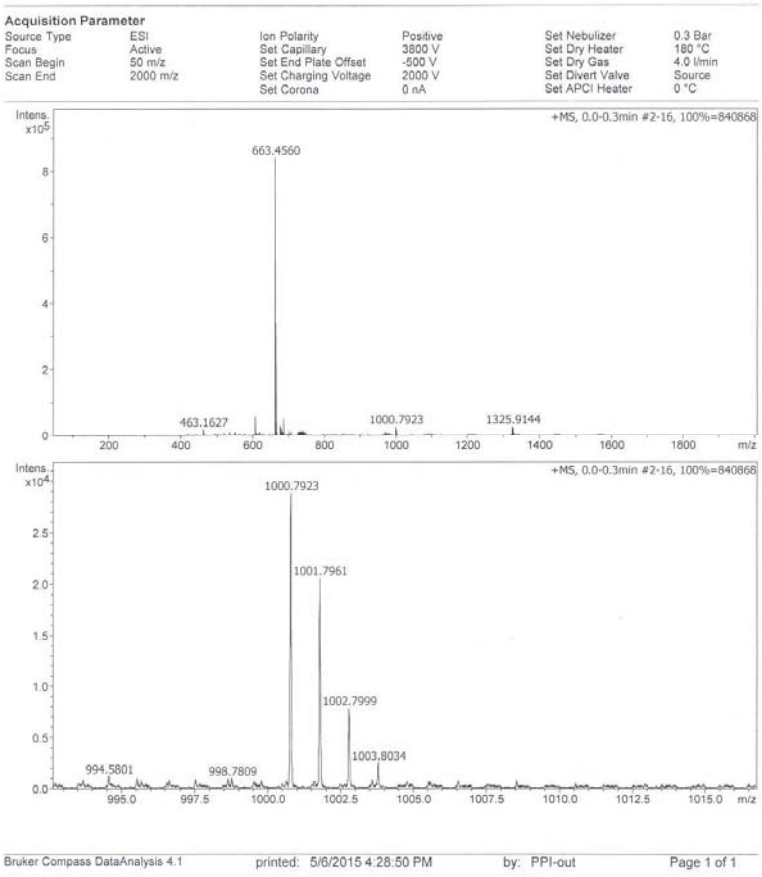

Fig.S5B: Mass spectroscopic data for the CB8-C7 system in solution at pH 3

However, we could not obtain the mass peaks for the contended 3:2 stoichiometry. We feel that this could be a practical issue such as the experimental instability of a 3:2 host guest stoichiometry in the gas phase during the ionization process in the mass spectrometer rather than the solution phase where we performed the photophysical measurements. For the monocationic form, the cationic charge resides on the benzimidazole/N-methylbenzimidazole moiety of C7/C30 dyes. The formation of 1:2 CB8:C30 complex is, therefore, driven by ion-dipole interaction of the cationic part of the guest dye with the partially negatively polarized carbonyl portal of the CB8 host. However, the interaction of two more CB8 hosts at both the ends of the 1:2 complex in forming the 3:2 complex is mainly supported by the hydrophobic interactions of the cavity in the aqueous environment. In the mass spectrometer environment, the ion dipole interaction between two species becomes stronger and the hydrophobic interactions weakens while lifting the $(CB8)_3.(C30)_2$ from the aqueous environment to gas phase. We believe that the non appearance of the expected mass peaks could be due to this practical issue. The importance of these contrasting features of ion dipole and hydrophobic interactions of supramolecular complexes in a mass spectrometric environment are discussed in detail in a recent literature (*ref*. M. Kogej and C. A. Schalley in '*Analytical Methods in Supramolecular Chemistry'*, 2007, page 104-159).

Note S5: *Computational details:*

All semi-empirical geometry optimization and energy minimization calculations were performed with PM7 Hamiltonian on MOPAC 2012; Version 15.089L and the optimized structures are shown in (Fig.S6). The localized molecular orbital method that was developed to enable calculation on large molecular systems and implemented on MOPAC2012 with keyword MOZYME was applied. To mimic the experimental conditions these calculations were performed with the continuum salvation model 'COSMO' with the dielectric constant set to 78.4.

Binding energies were calculated with the equation

$$\Delta H_{binding} = \Delta H_{complex} - n(\Delta H_{f\,CB8}) - n(\Delta H_{f\,guest\ dyes})$$

where, n is the number of molecules involved in complex formation.

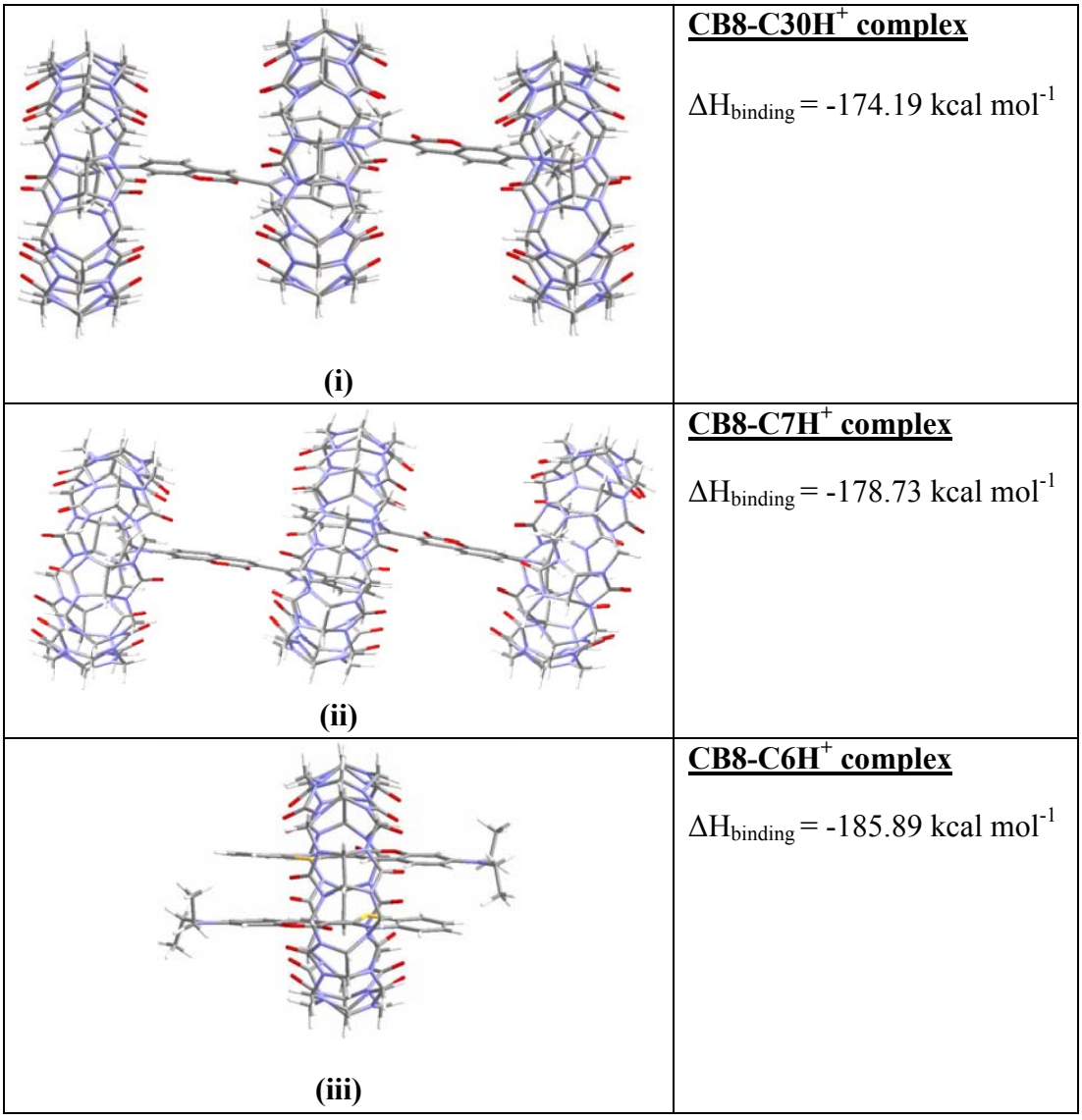

Fig. S6: Geometry optimized structural arrangement for the CB8:Dye complexes, in 3:2 stoichiometry for $C30H^+$ (**i**), $C7H^+$ (**ii**) and 1:2 stoichiometry for $C6H^+$ (**iii**).

Note S6: *Measurement of quantum yields and the calculation of Slip Angle θ:*

Emission quantum yield (Φ) measurements were carried out using EDINBURGH instrument model FLS920 equipped with 450W Xenon arc lamp having Peltier element cooled red sensitive Hamamatsu R955 PMT. Quantum yield of the samples were calculated based on the absolute method using integrating sphere of diameter 15 cm coated with $BaSO_4$ after standardization. The performance of the integrating sphere was verified by using rhodamine B as test sample. The absolute quantum yield was calculated for rhodamine B first and compared with its literature value (0.21) in water, which matched very well. It was assumed that light falling to $BaSO_4$ coating are scattered perfectly (100%). Sample holder is kept in the centre of sphere and scattered light was collected by detector through two windows: one for entrance of exciting light and another for collection of scattered/emitted light.

Emission quantum yield (Φ) is related to number of photons absorbed (α) and number of photons emitted by the sample (ε) as

$$\Phi = \frac{\varepsilon}{\alpha} = \frac{\int I_{Emission}}{\int I_{Solvent} - \int I_{Sample}}$$

where, $I_{emission}$ is emission spectrum of sample, $I_{solvent}$ is the spectrum of light used to excite only solvent (water) and I_{sample} is the spectrum of light used for exciting sample (C30.CB8 or C7.CB8 complexes) in solvent. In the present case samples were excited at 450nm and emission spectrum were collected from 461nm to 750nm with minimum slit width. All spectrums were corrected with the correction factor for the integrating sphere before calculation of the quantum yields.

Based on McRae and Kasha's theory the geometric arrangement of molecules in dimeric state may be evaluated by measuring the excites state lifetimes which is expressed as

$$k_{rD} = 2k_{rM}\cos^2\theta$$

where k_{rD} and k_{rM} are the radiative rate constants of the dimer and the monomer respectively and θ is the angle between the transition dipole moment and the line joining the two molecular centres of the dimer. The radiative rate constants can be calculated from the knowledge of the quantum yields and the excited state lifetimes of the respective species as

$$k_f = \Phi/\tau$$

These important parameters thus evaluated are compiled in Table S2.

Table S2: *Absolute fluorescence quantum yield estimated and the slip angle (θ) calculated for the C30 and C7 dyes in presence of CB8.*

System	Φ_f **absolute.**	k_{rD} **($10^7 s^{-1}$)**	k_{rM} **($10^8 s^{-1}$, for free dye)**	θ *(from* McRae and Kasha's theory*)*	θ *(from optimized geometry)*
CB8-C30	0.29	1.49	1.73	12°	16°
CB8-C7	0.20	2.04	1.11	18°	22°
CB8-C6	0.1	0 (no dimer emission)	2.5	---	87°

Note S7: *Control studies of interaction of C30 and C7 dye with γ-Cyclodextrin hosts in aqueous solution at pH3*

To demonstrate the unique ability of CB8 host to template a homodimeric association of bichromophoric coumarin derivatives C30 and C7 leading to hitherto unknown excimer emission, a comparative study was carried out to evaluate such possibility of eximer formation of these dyes in receptor host with comparative cavity size namely, γ-cyclodextrin under similar experimental condition. As shown in the Fig. S7(A), with increase in the concentration of γ-cyclodextrin, the steady-state absorption profile of C30 dye in aqueous solution at pH 3 displayed a nominal decrease in the absorption with no change in the position of the maximum. However, the corresponding emission profile apparently did not display any change (Fig.S7(B)). On the other hand, as shown in the Fig.S7(C) & (D), C7 dye also displayed a very similar trend along with negligible quenching of emission intensity with increasing concentration of γ-cyclodextrin in aqueous solution at pH3. These observations indicate that the interaction of monocationic C30 and C7 dye with γ-cyclodextrin is negligibly weak and no indication of dimer formation was detected under experimental conditions.

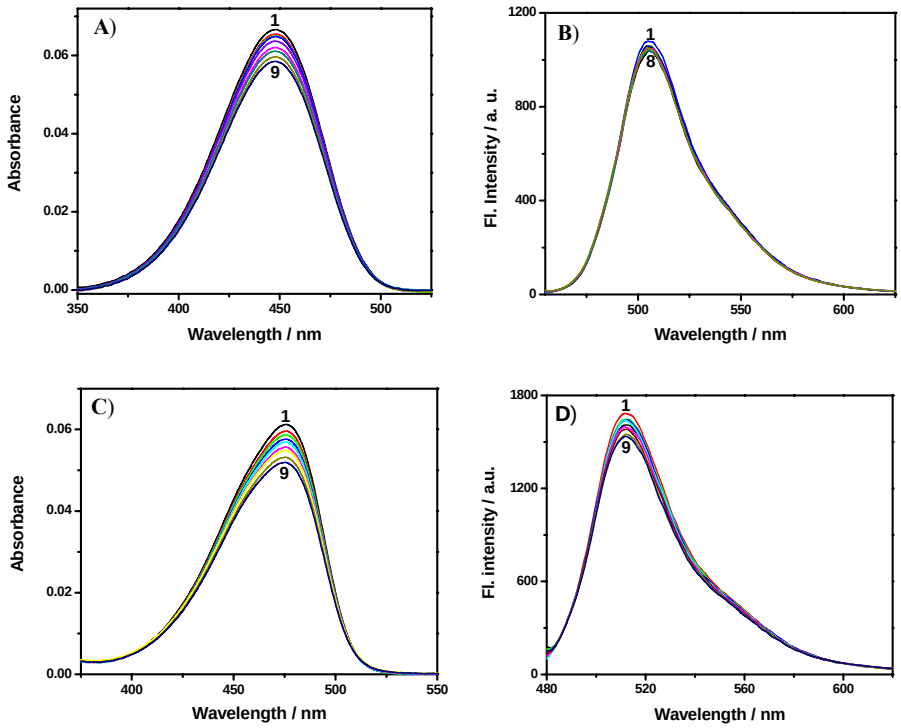

Fig.S7: (A) Steady-state absorption spectroscopic profile of free C30 dye (1) and in presence of 1mM γ-cyclodextrin (9); B) Emission spectral changes in of free C30 dye (1) and in presence of 0.8mM γ-cyclodextrin (8) in aqueous solution at pH3. **(**C) Steady-state absorption spectroscopic profile of free C7 dye (1) and in presence of 1mM γ-cyclodextrin (9); (D) Emission spectral changes in of free C7 dye (1) and in presence of 1mM γ-cyclodextrin (9) in aqueous solution at pH3.

Note S8: *Determination of binding constants of C30, C7 and C6 dye with CB8 host in aqueous medium at pH3*

A) Isothermal Calorimetric (ITC) titration for for CB8-C30H$^+$ host-guest system:

Based on the ^{1}H-NMR spectroscopic evidences and Jobs plot, we assumed 3:2 CB8:C30 stoichiometry with protonated N-methylbenzimidazole and 7-N,N′-diethyl amino groups as two binding sites. Therefore, a sequential two-site binding model is used to fit the ITC data and respective analysis is shown below.

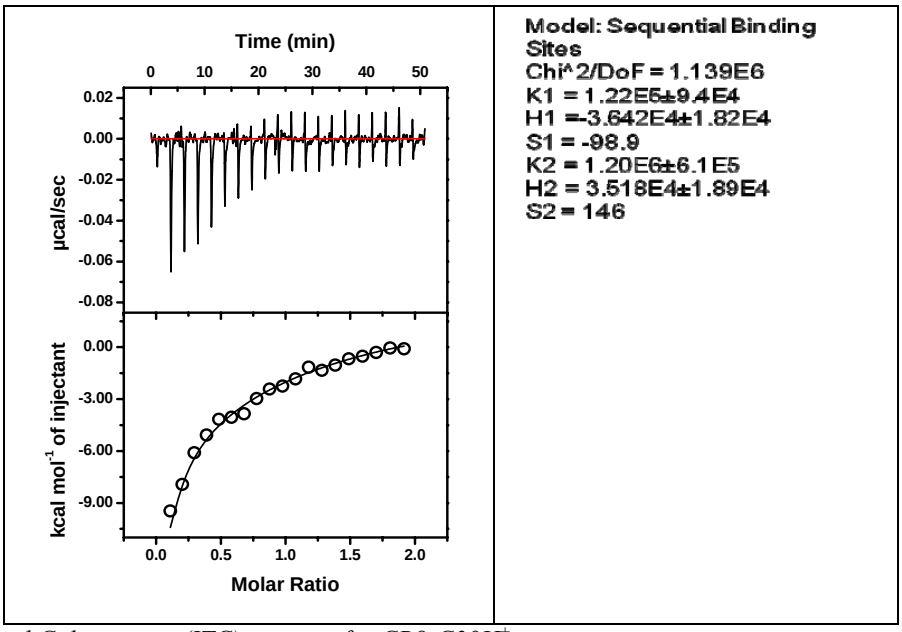

Fig.S8: *Isothermal Calorimetric (ITC) titration for CB8-C30H*$^{+}$

B) Isothermal Calorimetric (ITC) titration for CB8-C7H^{+} *host-guest system:*

As in the previous case for C30.CB8 system, the ITC data for C7.CB8 titration were fitted with a sequential two-site binding model and the thermodynamic data were evaluated as described below.

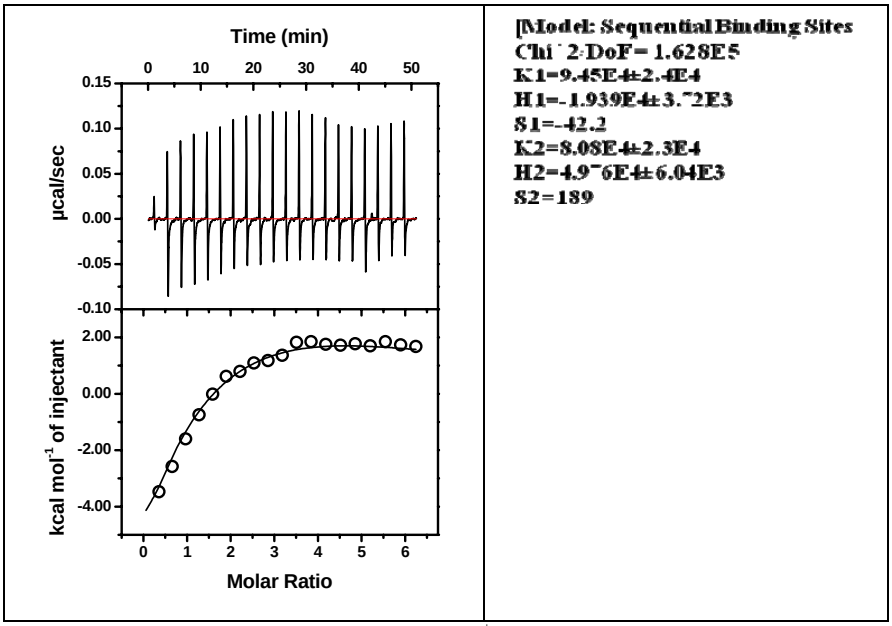

Fig.S9: *Isothermal Calorimetric (ITC) titration for CB8-C7H*$^{+}$ *host-guest system*

C) Determination of host-guest association constant for CB8-C6H$^+$ host-guest system:

Due to the lack of adequate ITC titration data, the association constant for C6H$^+$ dye with CB8 was evaluated based on fluorescence measurements.

Considering a 1:2 host-guest stoichiometry for CB8.C6H$^+$ system, the complexation equilibrium can be expressed as

$$2C6H^+ + CB8 \overset{K_{obs}}{\rightleftharpoons} (C6H^+)_2.CB8$$

and the observed binding constant (K_{obs}) can be expressed as $K_{obs} = \frac{[(C6H^+)_2.CB8]}{[C6H^+]^2 \times [CB8]}$

If 'a' is the concentration of the guest C6H$^+$ in absence of CB8 host and 'b' is the concentration of the host CB8 with respect to the 50% of the total change in monitoring parameter (in this case fluorescence intensity) then,

$$K_{obs} = \frac{(a/2n)}{\{(a/2)^n \times b\}}$$

Following the above equation the estimated overall binding constant ($K=K_1 \times K_2$) for C6H$^+$.CB8 system is $8.3 \times 10^{11} M^{-2}$.